J. Fluid Mech. (2019), *vol.* 876, R2, doi:10.1017/jfm.2019.586

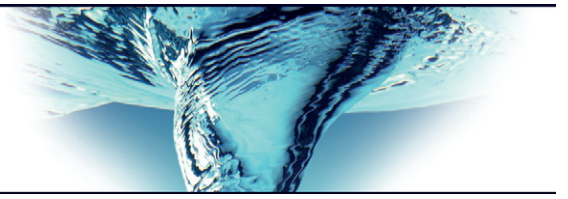

JFM RAPIDS
journals.cambridge.org/rapids

Flight-crash events in superfluid turbulence

P. Švančara[1] **and M. La Mantia**[1,†]

[1]Faculty of Mathematics and Physics, Charles University, Ke Karlovu 3, 121 16 Prague, Czech Republic

(Received 20 May 2019; revised 13 July 2019; accepted 16 July 2019; first published online 1 August 2019)

We show experimentally that the mechanisms of energy transport in turbulent flows of superfluid ^{4}He are strikingly different from those occurring in turbulent flows of viscous fluids. We argue that the result can be related to the role played by quantized vortices in this unique type of turbulence. The flow-induced motions of relatively small particles suspended in the liquid reveal that, for scales of the order of the mean distance between the vortices, the particles do not tend on average to decelerate faster than they accelerate, whereas, at larger scales, a classical-like asymmetry is recovered. It follows that, in the range of investigated parameters, flight-crash events are less apparent than in classical turbulence. We specifically link the outcome to the time symmetry of quantized vortex reconnections observed at scales comparable to the typical particle size.

Key words: particle/fluid flows, quantum fluids, turbulent flows

1. Introduction

Particles probing turbulent flows of viscous fluids tend to gain energy less quickly than they lose it, at all probed scales (Xu *et al.* 2014). The outcome has been related to the occurrence of flight-crash events, meaning that particles decelerate on average faster than they accelerate, and provides clear evidence, from a Lagrangian viewpoint, that classical turbulent flows are time irreversible – that is, it shows that the energy put into the system is eventually dissipated by the action of the fluid viscosity (Pumir *et al.* 2016).

We report here our experimental investigations on the occurrence of flight-crash events in turbulent flows of superfluid ^{4}He (He II), which is a quantum liquid characterized by unique properties, such as an extremely small kinematic viscosity (Barenghi, Skrbek & Sreenivasan 2014; Mongiovì, Jou & Sciacca 2018). Above 1 K, as in the present study, He II can be adequately modelled by assuming that it is made of two fluids, the viscous (normal) component and the inviscid superfluid, with the density ratio between the components being strongly temperature-dependent.

† Email address for correspondence: lamantia@mbox.troja.mff.cuni.cz

Additionally, turbulent flows of He II are defined by the presence of tangles of quantized vortices, which are line singularities within the fluid and can be viewed as the carriers of the flow vorticity. Indeed, it has been shown that, in the range of investigated parameters, quantum features are apparent at scales smaller than the mean distance between the vortices, regardless of the type of investigated flow, whereas, at larger scales, a classical-like behaviour is observed, within the Lagrangian framework (La Mantia *et al.* 2016; Švančara & La Mantia 2017).

Due to the presence of quantized vortices, energy transport mechanisms in turbulent flows of He II are therefore expected to be different from those occurring in similar flows of viscous fluids – as discussed, for example, by Clark di Leoni, Mininni & Brachet (2017). There is specifically numerical evidence that, when the normal component is absent (that is, when the fluid viscosity is null), the energy put into the system is dissipated by sound emission, following vortex reconnections and excitation of Kelvin waves. However, above 1 K, in the two-fluid regime of He II, the liquid viscosity, carried by the normal component, cannot be neglected and it should then play a role in the mechanisms of energy dissipation, although its relevance has yet to be clarified.

We consequently decided to verify this long-held expectation by experimentally looking for signatures of flight-crash events. Relatively small solid particles are suspended in the liquid and illuminated by a planar laser sheet. The flow-induced particle motions are then collected by a digital camera and processed by using the Particle Tracking Velocimetry technique (see, for example, Guo *et al.* 2014). We specifically calculate the velocity increments along the particle trajectories, introduced by Lévêque & Naso (2014), and the skewness of the corresponding statistical distributions, which, in homogeneous and isotropic turbulence, was found to be negative at all probed scales, indicating that particle deceleration is on average more abrupt than acceleration.

The obtained results strongly suggest that, in turbulent flows of superfluid ^{4}He, flight-crash events are less apparent than in classical turbulence, at least for scales of the order of the mean distance ℓ between quantized vortices, whereas, at larger scales, the flow behaviour is classical-like; that is, the skewness of the particle velocity increment distributions is neatly negative only in the latter case. The outcome therefore indicates that the action of the fluid viscosity (that is, of the fluid normal component) is mostly relevant at scales appreciably larger than ℓ, whereas at smaller scales, energy transport is instead ruled by the dynamics of the quantized vortex tangle.

2. Methods

Both thermally and mechanically driven flows of He II are investigated. The latter is generated by two square grids oscillating vertically in phase (Švančara & La Mantia 2017) and the former by a flat heater placed at the bottom of a vertical channel of square cross-section, resulting in the so-called thermal counterflow of superfluid helium (Mongiovì *et al.* 2018). Once the heater is switched on or the grids are set into motion, the particles suspended in the bath move on average in the vertical direction and their dynamics is appreciably affected by the quantized vortex tangle, especially at scales smaller than ℓ (La Mantia *et al.* 2016).

For the thermal counterflow experiments reported here we use solid deuterium hydride particles, which have sizes of a few micrometres. Their flow-induced motions are visualized in a region approximately 1 mm thick, 13 mm wide and 8 mm

high, situated sufficiently away from the flow source, in the middle of our glass channel, of 25 mm sides and 10 cm high. Considering that the flow mean direction is perpendicular to our flat heater, it is not expected that significant flows occur in planes parallel to the heat source (that is, perpendicular to the field of view), especially away from the channel walls, as in the present case; see Švančara *et al.* (2018) for further details on the counterflow setup.

Additionally, it is important to highlight that the present counterflow data are obtained in the turbulent state – that is, at fluid velocities appreciably larger than the turbulence onset velocity, equal to approximately 1 mm s^{-1} for our channel (La Mantia 2016). In this regime the particles move on average upward, away from the heater, and their trajectories do not follow straight lines, indicating that particle motions are affected by the presence of quantized vortices; see, for example, La Mantia (2016) for a discussion on the particle behaviour in different counterflow conditions.

Deuterium particles of similar sizes are employed for the oscillating grid experiments (Švančara & La Mantia 2017) and the studied flow region has dimensions comparable to the counterflow one. It is located between the grids, as far away as possible from the solid boundaries of the experimental volume, of 50 mm sides (the fixed distance between the grids is 70 mm). It follows that, also in this case, significant flows perpendicular to the field of view (that is, parallel to the horizontal flow generator) are not expected to occur. Thermal counterflow (oscillating grid) movies are collected at 500 (400) fps. Once particle positions are obtained from the movies, the corresponding particle velocities and velocity increments are computed as in previous studies (see, for example, Švančara *et al.* 2018).

Following Lévêque & Naso (2014) we focus our attention here on the longitudinal velocity increments, computed along the particle trajectories. Each increment $\mathrm{d}v(\tau)$ is computed as the scalar product of two vectors, the Cartesian velocity increment and the corresponding position increment; τ indicates the time lag between the considered velocities and positions. The normalized skewness Sk of the $\mathrm{d}v$ statistical distribution is obtained as

$$Sk(\tau) = \frac{\langle [\mathrm{d}v(\tau) - \mathrm{d}v_m(\tau)]^3 \rangle}{\mathrm{d}v_{sd}(\tau)^3} = \frac{Sk_d(\tau)}{\mathrm{d}v_{sd}(\tau)^3}, \tag{2.1}$$

where the symbols with subscripts m and sd denote the mean and standard deviation of the velocity increment ensemble $\langle \mathrm{d}v(\tau) \rangle$ at time lag τ, respectively.

3. Results

In figure 1 we plot Sk as a function of the time ratio $t_R = \tau/\tau_f$, where τ_f indicates a relevant flow time scale, equal to the Kolmogorov time scale τ_η for the classical data (Lévêque & Naso 2014). In the case of the He II turbulent flows we follow La Mantia & Skrbek (2014), and set $\tau_f = \tau_\ell$, the time needed to travel a distance equal to ℓ with the mean particle velocity V, obtained at the smallest time τ_{min} between particle positions (that is, the time between consecutive images).

For the thermal counterflow data we estimate the mean distance between quantized vortices following the procedure outlined by Švančara *et al.* (2018) – that is, from the flatness of the particle velocity distributions. The obtained ℓ values are listed in table 1 together with other relevant quantities. For the oscillating grid data we employ the ℓ values estimated by Švančara & La Mantia (2017) (see also table 2).

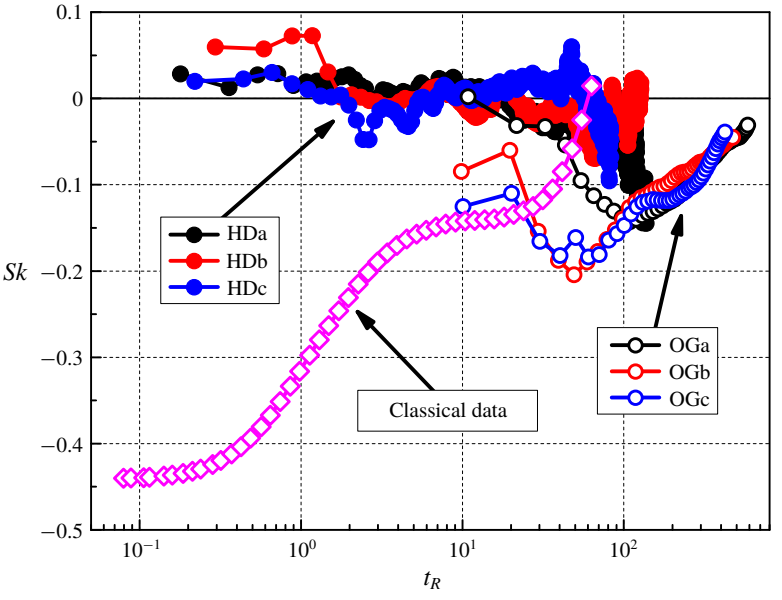

FIGURE 1. Normalized skewness Sk of the longitudinal velocity increment distribution as a function of the time ratio t_R, see (2.1). Filled and open circles indicate thermal counterflow and oscillating grid data, respectively; relevant experimental parameters are listed in tables 1 and 2; at least 10^5 velocity increments are employed for each experimental point. The open diamonds denote the classical data, obtained at a Taylor-based Reynolds number R_λ equal to 280 (Lévêque & Naso 2014); note that, for the oscillating grid experiments, $R_\lambda \approx 300$ (Švančara & La Mantia 2017).

Data set	T	q	V	ℓ	τ_ℓ
HDa	1.50	193	3.1	35	11.2
HDb	1.50	349	4.6	31	6.8
HDc	1.76	616	3.0	27	9.1

TABLE 1. Thermal counterflow experimental conditions: temperature T, in K; applied heat flux q, in W m^{-2}; mean particle velocity V, in mm s^{-1}, at the smallest time τ_{min} between particle positions; mean distance ℓ between quantized vortices, in μm, estimated following the procedure outlined by Švančara *et al.* (2018); time τ_ℓ, in ms, needed to travel a distance equal to ℓ with a velocity V.

It is apparent from figure 1 that the results obtained in He II are strikingly different from the classical one, especially at the smallest scales, of the order of τ_ℓ. At larger scales, for $t_R > 10$, the trend observed for the oscillating grid data appears instead to be consistent with the classical behaviour.

In order to appreciate the latter outcome we employ the dimensional value of Sk – that is, the numerator of (2.1) – and we plot in figure 2(*a*) the magnitude of Sk_d, in mm^3 s^{-3}, as a function of t_R; note that for the classical data the investigated flow has zero mean velocity and that the corresponding root mean square (r.m.s.) velocity is equal to 145 mm s^{-1}.

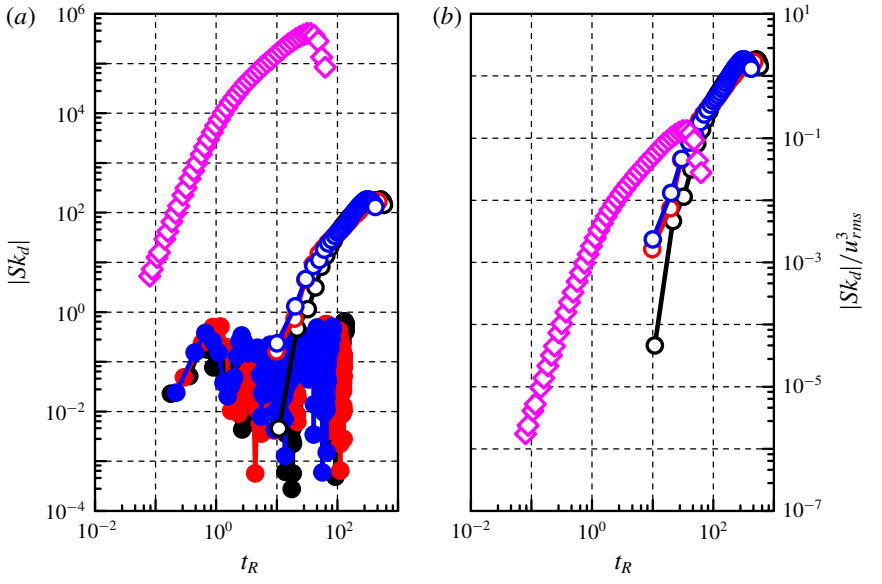

FIGURE 2. (*a*) Absolute value of the dimensional skewness Sk_d, in mm^3 s^{-3}, as a function of t_R, see (2.1). (*b*) Absolute value of Sk_d, normalized by using the root mean square value u_{rms} of the fluid velocity, as a function of t_R; u_{rms} is equal to 145 mm s^{-1} in the classical case and is set to $100^{1/3}$ mm s^{-1} for the grid experiments. Symbols as in figure 1 in both panels.

Data set	T	V	ℓ	τ_ℓ
OGa	1.95	22.4	5	0.2
OGb	1.75	20.0	5	0.3
OGc	1.50	20.9	5	0.2

TABLE 2. Oscillating grid experimental conditions: symbols as in table 1; ℓ was estimated by Švančara & La Mantia (2017), where further experimental details can be found. For all cases the oscillation frequency is 3 Hz and its amplitude 10 mm.

We clearly observe in figure 2 that our oscillating grid results and the classical data behave in a similar fashion; that is, they both follow, at large enough times, the scaling $|Sk_d| \propto t_R$ reported by Lévêque & Naso (2014). Additionally, taking into account that a Kolmogorov-like time scale suitable for the description of He II turbulent flows should be of the same order of the scale τ_ℓ employed here (as discussed, for example, by La Mantia (2017)), we can estimate the r.m.s. value of the fluid velocity for our grid experiments. If we set the latter to $100^{1/3}$ mm s^{-1}, the data neatly collapse, as shown in figure 2(*b*), where the chosen value is approximately four times smaller than the r.m.s. value of the particle velocity in the horizontal direction, which should be less affected by the imposed vertical motion. Considering the assumptions involved in the estimate, the displayed outcome is remarkable.

On the other hand, it is hard to deny that a striking difference between the counterflow results and the oscillating grid data is seen in figures 1 and 2. In order to highlight it we plot in figure 3 the dimensional skewness Sk_d as a function of t_R.

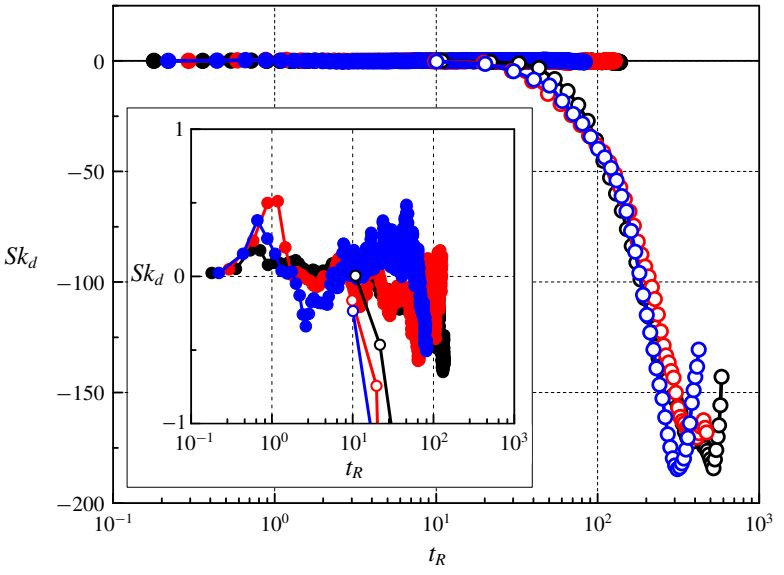

FIGURE 3. Dimensional skewness Sk_d, in mm^3 s^{-3}, as a function of t_R, see (2.1). The inset has different vertical axis extrema in order to highlight the thermal counterflow data. Symbols as in figure 1.

The outcome is also apparent if, following Xu *et al.* (2014) and Bhatnagar *et al.* (2018), we calculate the particle energy increments from their velocities. Indeed, for the skewness of the energy increments distribution, the obtained behaviour is very similar to that shown in figure 3 for Sk_d, if it is displayed in a similar fashion.

4. Discussion

It is now time to address the physical implications of the reported results. We start by noting that the numerical data discussed by Lévêque & Naso (2014) were obtained in three-dimensional homogeneous and isotropic turbulence, while the studied He II flows have a preferential direction of motion and are investigated in a planar region, parallel to the mean flow direction, placed as far away as possible from the experimental volume vertical walls. The obtained particle trajectories therefore occur in a plane; but, as mentioned above, we do not expect that the observed particle dynamics would be significantly affected if three-dimensional tracks were considered, due to the symmetry of the imposed flow geometries. Additionally, it has been recently reported that, for classical channel flows, the statistical distributions of particle longitudinal accelerations are characterized by negative skewness values at various distances from the wall (Stelzenmuller 2018). It then follows that the inhomogeneity and anisotropy of the He II flows studied here are likely not sufficient to explain the reported disagreement with respect to the classical numerical results. Similarly, we may also disregard the influence of the particle inertia because numerical evidence of flight-crash events has been found, in homogeneous and isotropic turbulence, not only for tracers (Lévêque & Naso 2014), but also for large buoyant bubbles (Loisy & Naso 2017) and inertial particles (Bhatnagar *et al.* 2018).

The present experimental results consequently suggest that particles probing turbulent flows of superfluid ^{4}He do not tend on average to accelerate less quickly

that they decelerate, if one consider scales of the order of the mean distance between quantized vortices (that is, for $t_R < 10$), whereas, at larger scales, we obtain a classical-like picture. The outcome could possibly be explained by taking into account that particles can probe individual reconnections of quantized vortices solely at sufficiently small scales (La Mantia *et al.* 2016). It then follows that, at larger scales, the particles not only sense the fluid viscosity but also probe the tangle collective behaviour, which have been both found to result in features similar to those observed in classical turbulent flows, at least within the Lagrangian framework.

To substantiate the claim we may proceed as follows. It has been reported a few times (see, for example, Zuccher *et al.* (2012) and Villois, Proment & Krstulovic (2017)), that, during reconnection, the quantized vortices approach is slower than the separation following the event. For viscous vortex reconnection the behaviour is qualitatively similar (Hussain & Duraisamy 2011), but the exponents of the corresponding time scalings are larger than in the quantum case. This could mean that viscous reconnections are faster, more powerful events than quantum ones.

The just-mentioned time asymmetry during reconnection implies that the initial energy carried by the vortices is not solely employed to drive the vortex motions after the event, but that it is also distributed to other processes, which, in the quantum case, can be identified with sound emission and excitation of Kelvin waves, whereas, in the classical case, these processes can be mostly related to the generation of vortical structures smaller than the original ones (see also McKeown *et al.* 2018).

However, in the quantum case, the asymmetry is solely apparent at scales larger than the vortex core size – approximately 10^{-10} m (Mongiovì *et al.* 2018) – but still significantly smaller than the typical dimension of our flow-probing particles, approximately 10^{-6} m. Indeed, it was reported, in both numerical simulations (Zuccher *et al.* 2012) and experiments (Paoletti, Fisher & Lathrop 2010), that, at the particle scale, the asymmetry is absent because the particles cannot sense phenomena happening at scales smaller than their size. The fact that, from the present experimental results, particles do not appear to decelerate faster than they accelerate could then be related to the time symmetry of quantum vortex reconnections at sufficiently large scales, but further investigations are required to verify the interpretation.

Additionally, as noted above, the thermal counterflow behaviour is different from that observed for the oscillating grid experiments. On the basis of, for example, figure 1, it could be argued that the two trends appear to join for $10 < t_R < 100$, but this should solely be regarded as a possibility needing further support. For example, one could start from the consideration that, in steady-state thermal counterflow, the vortex tangle is expected to be polarized in planes perpendicular to the mean flow direction (Mongiovì *et al.* 2018), while this should not be the case for the mechanically driven flow considered here (Švančara & La Mantia 2017).

5. Conclusions

Our experimental results clearly indicate that energy transport mechanisms in turbulent flows of superfluid ^{4}He are appreciably different from those occurring in similar flows of viscous fluids. We argued that the outcome may be related to the scale-dependent interactions between our flow-probing particles and quantized vortices. It can be said that, at large enough scales, the vortex tangle collective behaviour resembles the action of the classical viscosity, whereas, at smaller scales, we found experimental evidence that, for He II turbulent flows, the energy put into

the system is not dissipated as in classical turbulent flows, but by other processes, likely related to the occurrence of quantized vortex reconnections, probed by our particles.

Acknowledgements

We thank A. Naso and E. Lévêque for providing relevant data (Lévêque & Naso 2014). We are grateful to P. Hrubcová, M. Rotter and L. Skrbek for valuable help. We acknowledge the support of the Czech Science Foundation (GAČR) under grant no. 19-00939S.

References

Barenghi, C. F., Skrbek, L. & Sreenivasan, K. R. 2014 Introduction to quantum turbulence. *Proc. Natl Acad. Sci. USA* **111**, 4647–4652.

Bhatnagar, A., Gupta, A., Mitra, D. & Pandit, R. 2018 Heavy inertial particles in turbulent flows gain energy slowly but lose it rapidly. *Phys. Rev.* E **97**, 033102.

Clark di Leoni, P., Mininni, P. D. & Brachet, M. E. 2017 Dual cascade and dissipation mechanisms in helical quantum turbulence. *Phys. Rev.* A **95**, 053636.

Guo, W., La Mantia, M., Lathrop, D. P. & Van Sciver, S. W. 2014 Visualization of two-fluid flows of superfluid helium-4. *Proc. Natl Acad. Sci. USA* **111**, 4653–4658.

Hussain, F. & Duraisamy, K. 2011 Mechanics of viscous vortex reconnection. *Phys. Fluids* **23**, 021701.

La Mantia, M. 2016 Particle trajectories in thermal counterflow of superfluid helium in a wide channel of square cross section. *Phys. Fluids* **28**, 024102.

La Mantia, M. 2017 Particle dynamics in wall-bounded thermal counterflow of superfluid helium. *Phys. Fluids* **29**, 065102.

La Mantia, M. & Skrbek, L. 2014 Quantum, or classical turbulence? *Europhys. Lett.* **105**, 46002.

La Mantia, M., Švančara, P., Duda, D. & Skrbek, L. 2016 Small-scale universality of particle dynamics in quantum turbulence. *Phys. Rev.* B **94**, 184512.

Lévêque, E. & Naso, A. 2014 Introduction of longitudinal and transverse Lagrangian velocity increments in homogeneous and isotropic turbulence. *Europhys. Lett.* **108**, 54004.

Loisy, A. & Naso, A. 2017 Interaction between a large buoyant bubble and turbulence. *Phys. Rev. Fluids* **2**, 014606.

McKeown, R., Ostilla-Mónico, R., Pumir, A., Brenner, M. P. & Rubinstein, S. M. 2018 Cascade leading to the emergence of small structures in vortex ring collisions. *Phys. Rev. Fluids* **3**, 124702.

Mongiovì, M. S., Jou, D. & Sciacca, M. 2018 Non-equilibrium thermodynamics, heat transport and thermal waves in laminar and turbulent superfluid helium. *Phys. Rep.* **726**, 1–71.

Paoletti, M. S., Fisher, M. E. & Lathrop, D. P. 2010 Reconnection dynamics for quantized vortices. *Physica D* **239**, 1367–1377.

Pumir, A., Xu, H., Bodenschatz, E. & Grauer, R. 2016 Single-particle motion and vortex stretching in three-dimensional turbulent flows. *Phys. Rev. Lett.* **116**, 124502.

Stelzenmuller, N. 2018 A Lagrangian study of inhomogeneous turbulence PhD thesis, Université de Grenoble-Alpes.

Švančara, P., Hrubcová, P., Rotter, M. & La Mantia, M. 2018 Visualization study of thermal counterflow of superfluid helium in the proximity of the heat source by using solid deuterium hydride particles. *Phys. Rev. Fluids* **3**, 114701.

Švančara, P. & La Mantia, M. 2017 Flows of liquid ^{4}He due to oscillating grids. *J. Fluid Mech.* **832**, 578–599.

Villois, A., Proment, D. & Krstulovic, G. 2017 Universal and nonuniversal aspects of vortex reconnections in superfluids. *Phys. Rev. Fluids* **2**, 044701.

XU, H., PUMIR, A., FALKOVICH, G., BODENSCHATZ, E., SHATS, M., XIA, H., FRANCOIS, N. & BOFFETTA, G. 2014 Flight-crash events in turbulence. *Proc. Natl Acad. Sci. USA* **111**, 7558–7563.

ZUCCHER, S., CALIARI, M., BAGGALEY, A. W. & BARENGHI, C. F. 2012 Quantum vortex reconnections. *Phys. Fluids* **24**, 125108.